Electronic Supplementary Material (ESI) for ChemComm.

Electronic Supplementary Information

For

The anion-sensing polyanion: a molecular cobalt vanadium oxide as multi-anion sensor

Andrey Seliverstov,[a,b] *Johannes Forster,*[a,b] *Magdalena Heiland,*[a] *Johannes Unfried,*[b]
Carsten Streb[a,b]*

[a]Institute of Inorganic Chemistry I, Ulm University, Albert-Einstein-Allee 11, 89081 Ulm, Germany
[b] previous address:Department Chemistry and Pharmacy, Inorganic Chemistry II, Friedrich-Alexander-University Erlangen-Nuremberg, Egerlandstr. 1, 91058 Erlangen, Germany.
*Email: carsten.streb@uni-ulm.de, web: www.strebgroup.net

1. Instrumentation

X-ray diffraction: Single-crystal X-ray diffraction studies were performed on a Nonius Kappa CCD Single-crystal X-ray diffractometer equipped with a graphite monochromator using MoK$_\alpha$ radiation (wavelength λ(Mo*K*α) = 0.71073 Å).

FT-IR spectroscopy: FT-IR spectroscopy was performed on a Shimadzu FT-IR-8400S spectrometer. Samples were prepared as KBr pellets. Signals are given as wavenumbers in cm^{-1} using the following abbreviations: vs = very strong, s = strong, m = medium, w = weak and b = broad.

UV-Vis spectroscopy: UV-Vis spectroscopy was performed on a Shimadzu UV-2401PC spectrophotometer, Varian Cary 50 spectrophotometer or Varian Cary 5G spectrophotometer equipped with a Peltier thermostat. All systems were used with standard cuvettes (d = 10.0 mm).

Thermogravimetry analysis (TGA): TGA was performed on a Setaram Setsys CS Evo, 30 - 900°C at 10K/min, 50 mL/min air, Graphite crucible 0.5 mL.

Elemental analysis: Elemental analysis was performed on a Euro Vector Euro EA 3000 Elemental Analyzer.

Atomic absorption spectroscopy: Atomic absorption spectroscopy analysis was performed on a Perkin Elmer 5100 PC spectrometer.

Nuclear Magnetic Resonance Spectroscopy (NMR): ^{1}H-NMR spectra were recorded at 269.7 MHz on a JNM-EX270 FT NMR spectrometer (JEOL). The solvent was DMSO-d6, data is given as chemical shifts δ in ppm.

Electrospray ionization mass spectrometry (ESI-MS): ESI-MS measurements were performed on an ultra-high resolution time-of-flight (UHR-TOF) Bruker Daltonik maXis, an ESI-TOF-MS. Detection was in negative-ion mode and the source voltage was 4 kV. The flow rates were 500 µL/hour. The drying gas (N_2) was held at 180 °C. The machine was calibrated prior to every experiment by direct infusion of the Agilent ESI-TOF low concentration tuning mixture.

General remarks: All chemicals were purchased from Sigma Aldrich or ACROS and were of reagent grade. The chemicals were used without further purification unless stated otherwise. $(n\text{-}Bu_4N)_4[V_4O_{12}] \times 4H_2O$ was synthesized as reported in the literature.[S1]

2. Synthetic section: Synthesis of compound 1

Method 1:

$(n\text{-}Bu_4N)_4[V_4O_{12}]$ (200 mg, 146.5 mmol) was dissolved in DMF (2 mL) and added to a solution of $Co(AcO)_2{\cdot}4H_2O$ (18.2 mg, 73.1 mmol) in DMF (4 mL). Upon mixing, a spontaneous colour change from pink to emerald green was observed. The clear, green solution was stirred at room temperature for 2 h. The product was obtained a single crystalline material by diffusion of diethyl ether or ethyl acetate into the mother liquor.

Yield: 65 mg (52.4 mmol, 71.4 % based on Co). Elemental analysis in wt.-% for $C_{50}H_{111}N_3O_{14}V_4Co$ (calculated values in brackets): C 48.63 (48.39), H 9.25 (9.01), N 3.47 (3.39), V 16.58 (16.41), Co 4.48 (4.75). Characteristic IR-bands (in cm^{-1}): 2959 (m), 2874 (vs), 1474 (s), 1379 (m), 1167 (s), 1109 (vs), 1057 (m), 1030 (s), 941 (m), 821 (b), 750 (m), 648 (b).

Method 2:

$(n\text{-}Bu_4N)_4[V_4O_{12}]$ (200 mg, 146.5 mmol) was dissolved in DMF or MeCN (2 mL). The resulting solution was added to a solution of $Co(NO_3)_2{\cdot}6H_2O$ (21.3 mg, 73.0 mmol) in DMF or MeCN (4 mL), which resulted in a spontaneous colour change of the reaction mixture to dark green. After stirring at 60 °C overnight the mixture was allowed to cool to RT. The product was obtained as emerald green crystals by diffusion crystallization using EtAcO as diffusion solvent. Lower yields (*ca.* 30 %) were observed as ethyl acetate decomposition (to give the required acetate ions) seems to be the limiting factor.

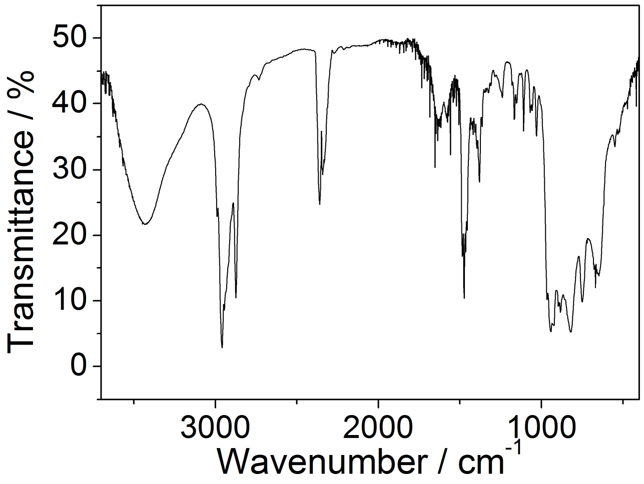

Figure S1: IR spectrum of compound 1.

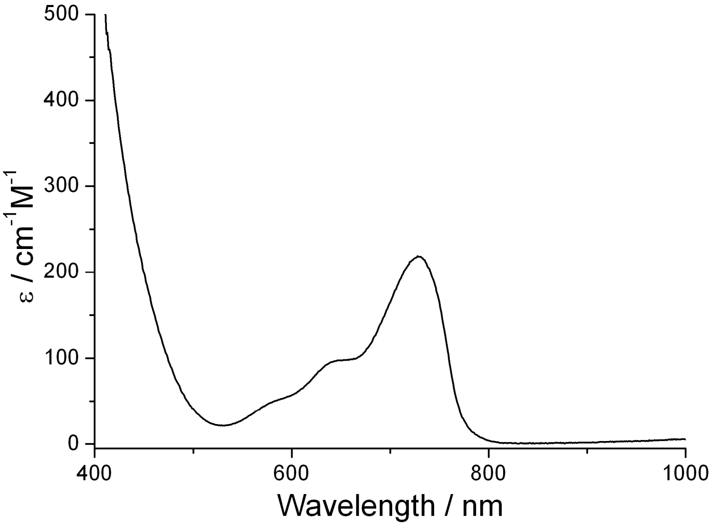

Figure S2: UV-Vis spectrum of **{CoV$_4$}** in DMF: λ_{max1} = 724 nm, ε = 242.7 M^{-1} cm^{-1}; λ_{max2} = 640 nm, ε = 120.0 M^{-1} cm^{-1}. λ_{max3} = 576 nm, ε = 71.2 M^{-1} cm^{-1}.

3. Crystallographic analysis of {CoV4}

Suitable single crystals of **1** were grown and mounted using a MicroLoop and Fomblin oil. X-ray diffraction intensity data were measured at 150 K on a Nonius Kappa CCD diffractometer [λ(Mo-K$_\alpha$) = 0.71073 Å] equipped with a graphite monochromator. Structure solution and refinement was carried out using the SHELX-97 package[S2] *via* WinGX.[S3] Corrections for incident and diffracted beam absorption effects were applied using empirical methods.[S4] Structures were solved by a combination of direct methods and difference Fourier syntheses and refined against F^2 by the full-matrix least-squares technique. Crystallographic data and structure refinements for compound **1**: $C_{50}H_{111}Co_1N_3O_{14}V_4$, M_r = 1241.11 g mol^{-1}; block crystal: 0.18 × 0.15 × 0.13 mm^3; T = 150(2) K. Monoclinic, space group $P2_1$, a = 11.8530(7), b = 21.6446(12), c = 12.5652(11) Å, β = 93.647(6), V = 3217.1(4) Å^3, Z = 2, ρ = 1.281 g cm^{-3}, μ(Mo$_{K\alpha}$) = 0.868 mm^{-1}, F(000) = 1326, 89091 reflections measured, 14733 unique (R_{int} = 0.0390), 659 refined parameters, R_1 = 0.0455, wR_2 = 0.1140. CSD 834843 contains the supplementary crystallographic data. These data can be obtained free of charge *via* www.ccdc.cam.ac.uk/conts/retrieving.html or deposit@ccdc.cam.ac.uk.

A suitable crystal of compound **2** was selected and mounted using a MicroLoop and Fomblin oil on a SuperNova, Dual, Cu at zero, Atlas diffractometer. The crystal was kept at 180.00(14) K during data collection. Using Olex2[S5], the structure was solved with the ShelXS structure solution program using Direct Methods and refined with the ShelXL[S2] refinement package using Least Squares minimization. Crystallographic data and structure refinements for compound **2:** $C_{55}H_{113}CoN_3O_{14}V_4$ (M =1303.17): monoclinic, space group Cc (no. 9), a = 24.1500(4) Å, b = 23.6855(4) Å, c = 23.9678(4) Å, β = 93.9267(14)°, V = 13677.5(4) Å^3, Z = 8, T = 180.00(14) K, μ(MoKα) = 0.820 mm^{-1}, *Dcalc* = 1.266 g/mm^3, 54985 reflections measured (6.16 ≤ 2Θ ≤ 65.598), 31955 unique (R_{int} = 0.0279, R_{sigma} = 0.0466) which were used in all calculations. The final R_1 was 0.0436 (I > 2σ(I)) and wR_2 was 0.1036 (all data).

Table S1. Crystal data and structure refinement compounds **1** and **2**

	Compound **1**	Compound **2**
Identification code	CCDC 834843	CCDC 1001987
Empirical formula	$C_{50}H_{111}CoN_3O_{14}V_4$	$C_{55}H_{113}CoN_3O_{14}V_4$
Formula weight	1241.11	1303.17
Temperature/K	150(2)	180.00(14)
Crystal system	monoclinic	monoclinic
Space group	$P2_1$	Cc
a/Å	11.8530(7)	24.1500(4)
b/Å	21.6446(12)	23.6855(4)
c/Å	12.5652(11)	23.9678(4)
α/°	90.00	90
β/°	93.647(6)	93.9267(14)
γ/°	90.00	90
Volume/$Å^3$	3217.1(4)	13677.5(4)
Z	2	8
ρ_{calc}mg/mm^3	1.281	1.266
m/mm^{-1}	0.868	0.820
F(000)	1326.0	5560.0
Crystal size/mm^3	0.25 × 0.18 × 0.16	0.2379 × 0.1958 × 0.1528
Radiation	MoKα (λ = 0.71073)	MoKα (λ = 0.71073)
2Θ range for data collection	6.62 to 55°	6.16 to 65.598°
Index ranges	$-15 \le h \le 15, -28 \le k \le 28, -16 \le l \le 16$	$-36 \le h \le 36, -35 \le k \le 35, -32 \le l \le 34$
Reflections collected	89091	54985
Independent reflections	14733 [R_{int} = 0.0390, R_{sigma} = 0.0330]	31955 [R_{int} = 0.0279, R_{sigma} = 0.0466]
Data/restraints/parameters	14733/1/659	31955/3829/1414
Goodness-of-fit on F^2	1.084	1.021
Final R indexes [I>=2σ (I)]	R_1 = 0.0455, wR_2 = 0.1101	R_1 = 0.0436, wR_2 = 0.0926
Final R indexes [all data]	R_1 = 0.0539, wR_2 = 0.1140	R_1 = 0.0633, wR_2 = 0.1036
Largest diff. peak/hole / e $Å^{-3}$	0.93/-0.50	0.35/-0.35
Flack parameter	0.012(15)	-0.018(5)

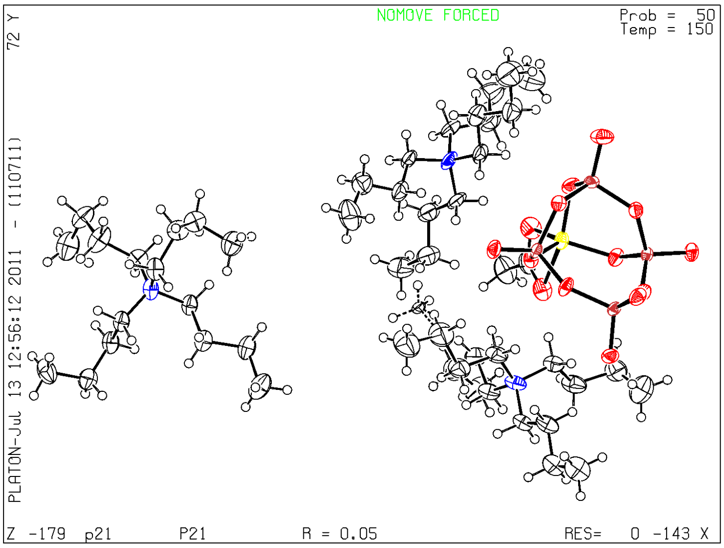

Figure S3: ORTEP representation of compound **1** (CCDC 834843), thermal ellipsoids given at 50 % probability.

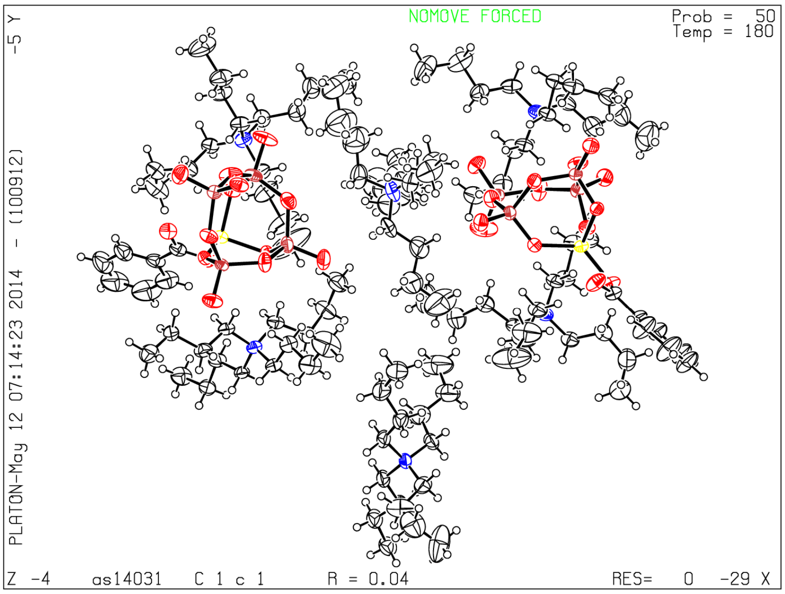

Figure S4: ORTEP representation of compound **2** (CCDC 1001987), thermal ellipsoids given at 50 % probability.

Compound $(n\text{-}Bu_4N)_3[CoV_4O_{12}Cl]$[S6] is registered under CCDC 721230.

4. NMR spectroscopy

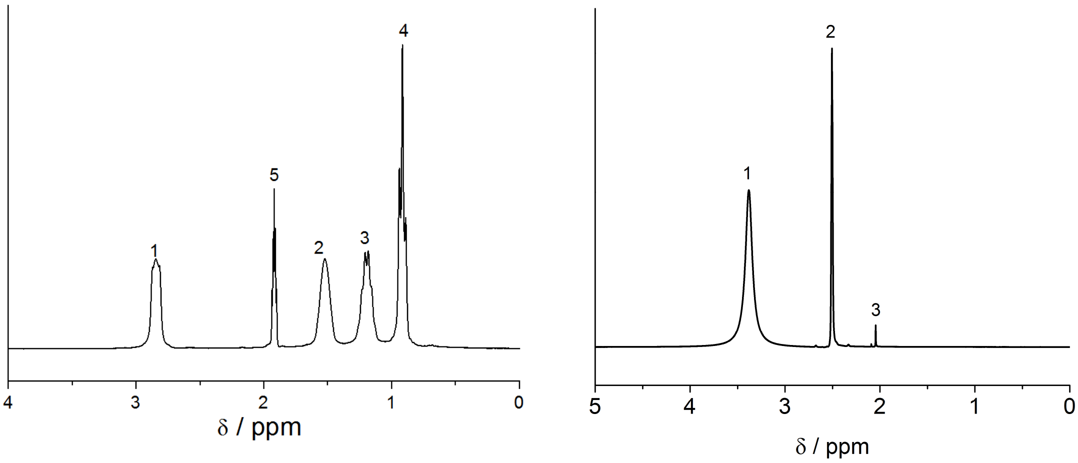

Figure S5: ^{1}H-NMR spectrum of **{CoV$_4$}** (left) and **Co(AcO)$_2$×6H$_2$O** (right) in DMSO-d6. See Table S2 for peak assignment. The AcO$^-$ methyl signal is observed at δ= 1.92 for **{CoV$_4$}** and at δ= 2.51 for Co(AcO)$_2$x6H$_2$O.

Table S2: **^{1}H-NMR peak assignment:**

δ / ppm	**Peak #**	**Peak assignment**	**No of H from integration (referenced to the *n*-Bu$_4$N - CH$_3$ group at 0.92ppm)**
		{CoV$_4$}	
0.92	**4**	N-CH$_2$-CH$_2$-CH$_2$-**CH$_3$**	<u>12.00</u>
1.20	**3**	N-CH$_2$-CH$_2$-**CH$_2$**-CH$_3$	8.16
1.52	**2**	N-CH$_2$-**CH$_2$**-CH$_2$-CH$_3$	8.04
1.92	**5**	**CH$_3$**-COO$^-$	3.12
2.85	**1**	N-**CH$_2$**-CH$_2$-CH$_2$-CH$_3$	7.08
		Co(AcO)$_2$×6H$_2$O	
2.09	**3**	**CH$_3$**-COO$^-$	
2.51	**2**	DMSO-d6	
3.38	**1**	**H$_2$**O	

5. ESI mass spectrometry

ESI mass spectrometry was performed in acetonitrile ([**1**] = 100 µM) in negative ion mode.

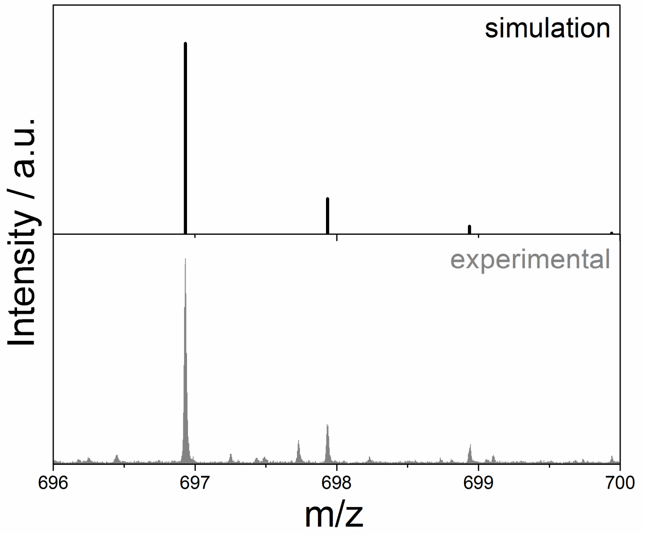

Figure S6: Experimental and simulated isotopic pattern of **1** with the loss of one acetate ligand. (n-Bu_4N)[CoV_4O_{12}]$^-$ at m/z = 696.9328.

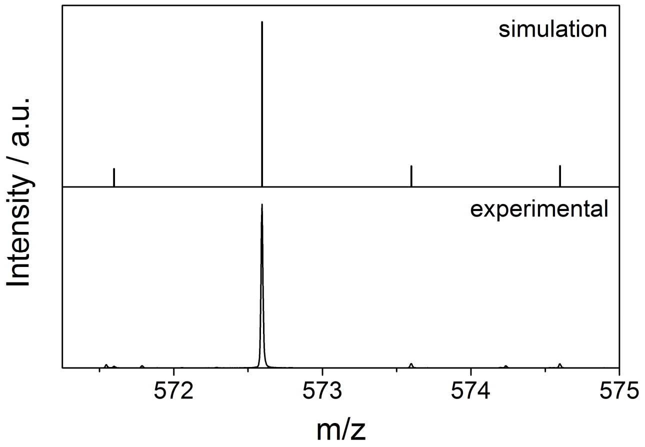

Figure S7: Experimental and simulated isotopic pattern of **1**: $Co^{II}[Co^{II}(AcO)V_4O_{12}]^-$ at m/z = 572.5946.

6. Thermogravimetric analysis

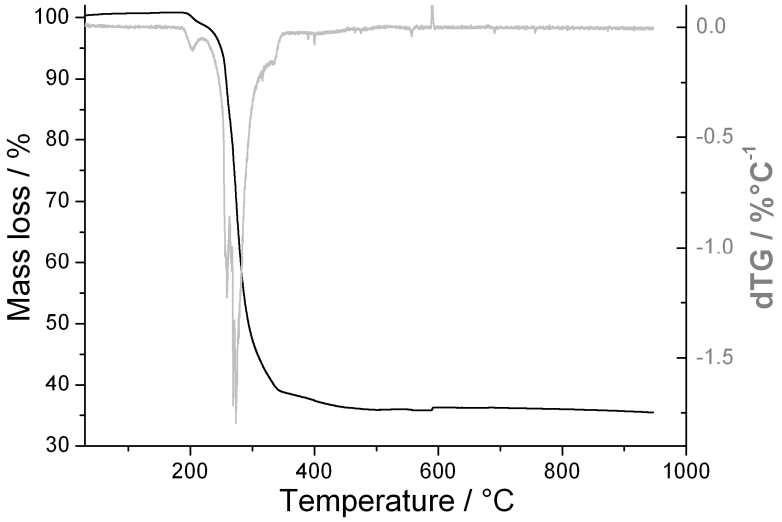

Figure S8: Thermogravimetric analysis of **{CoV$_4$}** showing one main mass loss step (exp: 64.1 wt.-%) between *ca*. 203 ˚C and *ca*. 500 ˚C, assigned to the loss of three *n*-Bu$_4$N$^+$ counterions (calcd. 58.6 wt.-%) and one acetate group (4.8 wt.-%, in sum 63.4 wt.-%). This is in line with the formula assigned from single-crystal XRD.

7. UV-Vis studies

7.1. Molar extinction coefficient of {CoV$_4$}

The molar extinction coefficients for **{CoV$_4$}** were determined by dissolving **{CoV$_4$}** in DMF solutions containing a large excess of acetate so as to drive the equilibrium fully to the **{CoV$_4$}** side. The experiment was conducted at several initial **{CoV$_4$}** concentrations and gave virtually identical molar extinction coefficients. Three d-d-transitions are observed at λ_1 = 576 nm (ε_{576} = 71.3 M^{-1} cm^{-1}), λ_2 = 640 nm (ε_{640} = 120.0 M^{-1} cm^{-1}) and λ_3 = 724 nm (ε_{724} = 242.7 M^{-1} cm^{-1}). For monitoring spectral changes upon acetate addition, the absorption signal a λ = 724 nm was used.

7.2 Co(NO$_3$)$_2$ / {V$_4$} titration series – acetate addition

For acetate-dependent sensor response studies, solutions of $Co(NO_3)_2$ × $6H_2O$ and **{V$_4$}** (molar ratio 1:1, [**{V$_4$}**]= 5 mM) were titrated with DMF-solutions of *n*-BuN$_4$(AcO) as acetate source.

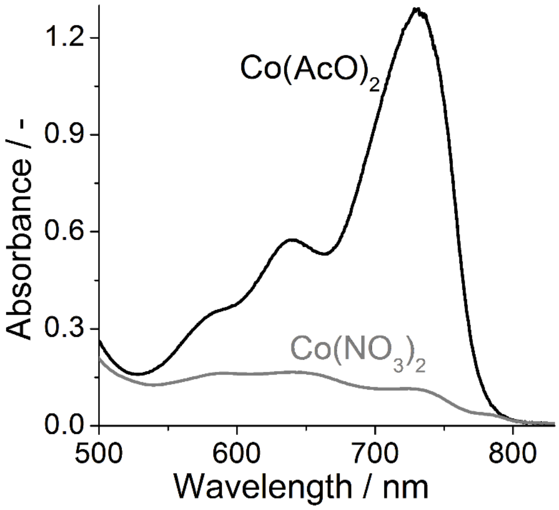

Figure S9: UV-Vis spectroscopic titration demonstrating the effect of acetate on the formation of **{CoV$_4$}** in solution. Various equivalents of acetate were added to solutions containing 1:1 molar ratios of [Co(NO$_3$)$_2$] / [**{V$_4$}**].

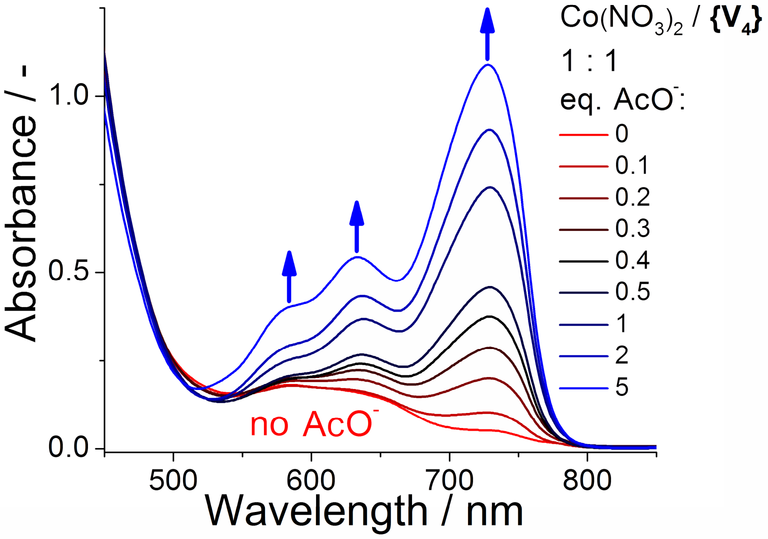

Figure S10: UV-Vis spectroscopic titration demonstrating the effect of acetate on the formation of **{CoV$_4$}** in solution. Various equivalents of acetate were added to solutions containing 1:1 molar ratios of [Co(NO$_3$)$_2$] / [**{V$_4$}**].

The effects of the **{V$_4$}** cluster on the spectral response to acetate-binding was studied using the reaction between acetate and a DMF solution of Co(NO$_3$)$_2$ × 6H$_2$O (5mM). The results show that acetate-binding also results in increased absorbance, however, in contrast to the **{CoV$_4$}** system, here, smaller changes in the molar extinction coefficients are observed together with an overall less characteristic spectral response, compare Fig. S8 and S9.

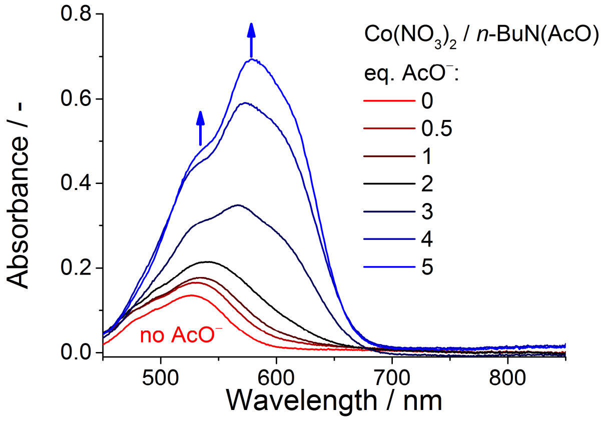

Figure S11: UV-Vis spectroscopic titration showing the spectral changes observed by addition of n-Bu$_4$N(AcO) to a DMF solution of Co(NO$_3$)$_2$ × 6H$_2$O (5mM).

The spectral response to chloride-binding was studied using the reaction between chloride and a DMF solution of **{V$_4$}** and Co(NO$_3$)$_2$ × 6H$_2$O (1:1, 5mM each). The results show that distinct spectral changes and increased absorbance are observed, these signals can be distinguished from acetate binding, see above.

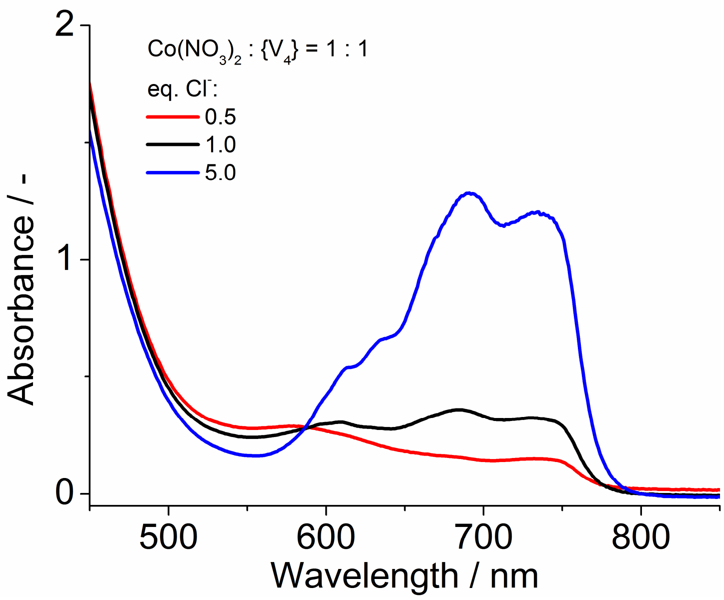

Figure S12: UV-Vis spectroscopic titration showing the spectral changes observed by addition of n-Bu$_4$NCl to a DMF solution containing 1:1 molar ratios of [Co(NO$_3$)$_2$] / [**{V$_4$}**] (5 mM).

7.3. Ratiometric behaviour

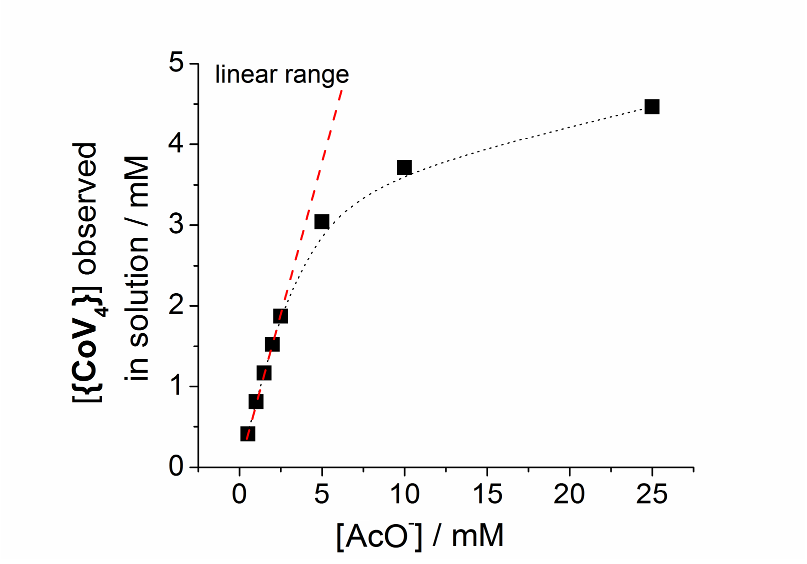

Figure S13: Linear ratiometric range of acetate detection showing the concentration of **{CoV$_4$}** in solution as a function of the acetate concentration. Linear range for acetate *ca.* 0.5 – 4 mM, [Co(NO$_3$)$_2$] = [**{V$_4$}**]= 5 mM.

7.4 {CoV_4} – addition of acetate

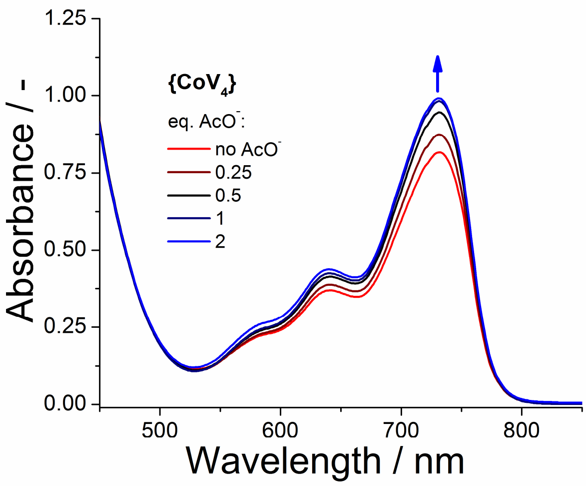

Figure S14: UV-Vis spectroscopic titration of acetate to a solution containing dissolved crystals of **{CoV_4}** ([**{CoV_4}**] = 10 mM in DMF). The data shows that upon dissolution, an equilibrium is obtained between **{CoV_4}** and non-cluster bound Co^{II} / **{V_4}** / AcO^-, see Scheme S1. Acetate addition shifts this equilibrium to the **{CoV_4}** side, thus higher **{CoV_4}** signal intensities are observed.

7.5 Solution equilibrium upon dissolving {CoV_4} in DMF

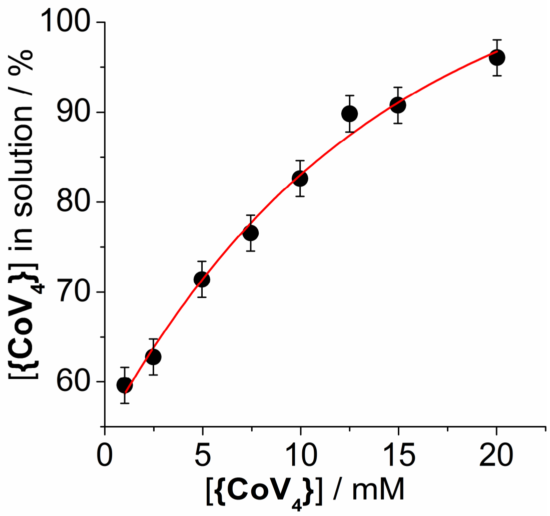

Figure S15: [**{CoV_4}**] observed in solution (solvent: DMF) as a function of the amount of **{CoV_4}** dissolved.

The dissociation constant K_d was calculated based on the following equation:

$K_d = [CoV_4O_{12}^{4-}] \times [AcO^-] / [Co(AcO)V_4O_{12}^{3-}]$

Equilibrium concentrations of the three components were determined photometrically using the known extinction coefficients.

$k_d^{60\%} = 2.78 \times 10^{-1}$ mM
$k_d^{95\%} = 3.23 \times 10^{-2}$ mM

7.6. Anion-selective spectral response of {CoV$_4$}

To investigate the anion-dependent behavior of **{CoV$_4$}**, DMF-solutions containing **{V$_4$}** (5 mM), $Co(NO_3)_2 \times 6H_2O$ (5 mM) and n-Bu_4NX ($x = PF_6^-$, $PhCOO^-$, Cl^-, [X] = 0.5 - 25 mM) were prepared and the spectral response to the anion was measured. As shown below, distinct spectral responses were observed for each anion, so that anion-selective detection becomes possible.

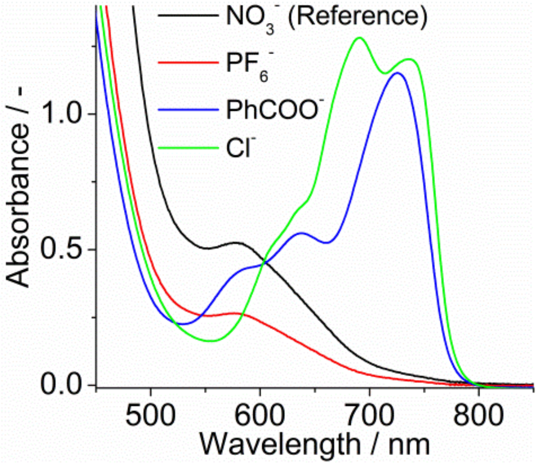

Figure S16: Spectral response of a 1:1 molar mixture of **{V$_4$}** and $Co(NO_3)_2 \times 6H_2O$ upon addition of 5 equivalents of the corresponding n-$Bu_4N(X)$ salt ($X = PF_6^-$, $PhCOO^-$, Cl^-), [X] = 25 mM. Solvent: DMF.

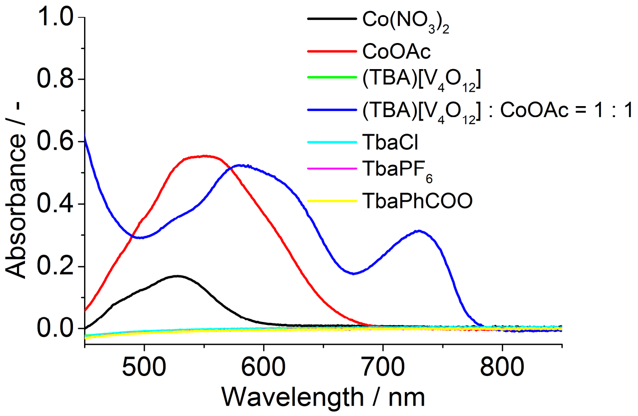

Figure S17: UV-Vis spectra of 5 mM solution of the educts and corresponding {CoV$_4$} solution in DMF. n-$Bu_4N(X)$ salts and {V$_4$} are not absorbing light at the given wavelength-area.

7.7. Thermal stability evaluation of {CoV$_4$}

The thermal stability of **{CoV$_4$}** was evaluated by heating a sample of **{CoV$_4$}** dissolved in DMF for 24 h to *T* = 90 ^{o}C. UV-Vis spectra were recorded before and after the heat treatment and virtually no changes to the characteristic UV-Vis signals of **{CoV$_4$}** can be observed, see below.

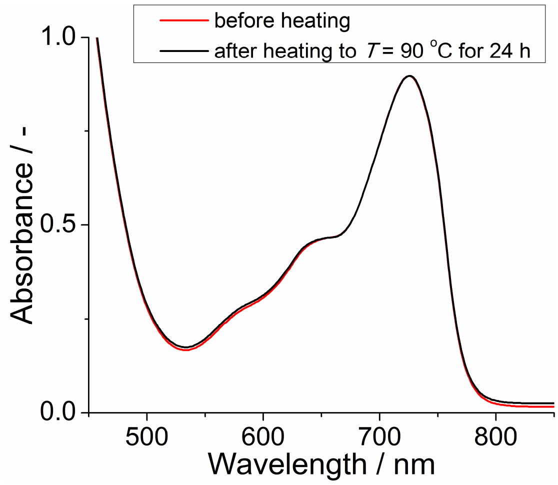

Figure S18: UV-Vis spectroscopic analysis of solution of {CoV$_4$} in DMF before (red line) and after (black line) heating the sample to *T* = 90 ^{o}C for 24 h.

8. Literature references cited in ESI

S1 J. Forster, J.; Rösner, B.; Khusniyarov, M. M.; Streb, C.; *Chem. Commun.*, **2011**, *47*, 3114.

S2 Sheldrick, G.M.; *Acta Crystallogr.* **2008**, *A64*, 112.

S3 Farrugia, L. J.; J. *Appl. Cryst*. **1999**, *32*, 837.

S4 Blessing, R. H.; *Acta Crystallogr.* **1995**, *A51*, 33.

S5 Dolomanov, O.V., Bourhis, L.J., Gildea, R.J, Howard, J.A.K. & Puschmann, H., *J. Appl. Cryst.* 42, **2009**, 339-341

S6 Kurata, T.; Hayashi, Y.; Isobe, K.; *Chem. Lett.* **2009**, 38, 218–219.